Ionospheric scintillation near the anomaly crest in relation to the variability of ambient ionization

S. K. Chakraborty,[1] R. Hajra,[1] and A. DasGupta[2]

Received 30 November 2011; accepted 9 February 2012; published 30 March 2012.

[1] Ionospheric scintillation near the anomaly crest is a matter of great concern for the design of transionospheric communication and navigation links and forecasting of the same is an important aspect of ensuing space weather scenario. Under present investigation, amplitude scintillation data at VHF/UHF, total electron content (TEC) data from Calcutta (geographic: longitude 88.38°E, latitude 22.58°N, dip: 32°N), situated virtually below the northern crest of equatorial ionization anomaly, are analyzed to study any correspondence between occurrences of postsunset equatorial scintillations and daytime ambient ionization characteristics. The study reveals distinctive features of diurnal TEC profiles on scintillation and non-scintillation days. The differences are reflected in daytime TEC parameters like diurnal peak values of TEC, its occurrence time, 3-dB width of diurnal TEC profile, daytime integrated TEC and average TEC level around the local sunset. The analysis reveals that local time of diurnal TEC maximum in conjunction with daytime integrated TEC values may potentially be selected to develop forecasting capability of postsunset scintillation for the equinoctial months of high solar activity years under quiet geomagnetic condition. The results are discussed in terms of sustenance probability of high ambient ionization in the postsunset period.

Citation: Chakraborty, S. K., R. Hajra, and A. DasGupta (2012), Ionospheric scintillation near the anomaly crest in relation to the variability of ambient ionization, *Radio Sci.*, *47*, RS2006, doi:10.1029/2011RS004942.

1. Introduction

[2] Two important aspects of the equatorial/low latitude ionosphere are the equatorial ionization anomaly (EIA) and the intense form of irregularities in electron density distribution. While the former develops mainly in the daytime hours, the later is mostly associated with the nighttime ionosphere. In daytime, the $\boldsymbol{E} \times \boldsymbol{B}$ upward vertical drift of plasma near the magnetic equator and subsequent diffusion along the magnetic field lines due to pressure gradient and gravitational forces develop the EIA. It is characterized by two crests of ambient ionization around ± 15–20° magnetic latitude and a trough at the magnetic equator. The diurnal pattern of development and decay of EIA depends on the phases of solar cycle as well as on the seasons. The dynamo electric field which is eastward during daytime and westward at night is mainly responsible for the EIA. The eastward electric field before reversal exhibits an enhancement in the postsunset period, known as prereversal enhancement (PRE) [*Rishbeth*, 1971; *Farley et al.*, 1986; *Crain et al.*, 1993; *Park et al.*, 2010]. It is related to F region dynamo. The detailed physical processes concerning the F region dynamo and PRE appear to be complicated and several explanations have been proposed [*Rishbeth*, 1971; *Farley et al.*, 1986; *Haerendel and Eccles*, 1992; *Prakash et al.*, 2009].The time and magnitude of PRE depend on the solar and magnetic activities, seasons and longitudes [*Fejer et al.*, 1991; *Abdu et al.*, 1995; *Kil and Oh*, 2011]. It is manifested by a resurgence-like feature in the EIA. It halts the normal decay to produce a secondary ledge in the ambient ionization [*Anderson and Klobuchar*, 1983]. A feedback mechanism between a fairly strong EIA at 1700 LT (local time) and PRE is also suggested to operate [*Prakash et al.*, 2009].

[3] Equatorial electron density irregularities of various scale sizes, commonly known as equatorial spread-F (ESF), are the other distinguishing features of equatorial ionosphere. At the magnetic equator around sunset, the F layer may rapidly rise and develop a steep bottom side gradient due to the combined effects of recombination of the F_1 and E layers and an actual increase in the vertical plasma velocity due to PRE. These conditions result in an F layer plasma density profile which is unstable to the Rayleigh-Taylor (R-T) instability [*Ossakow*, 1981]. Onset of this instability results in upwelling of low-density bottom side plasma, known as bubbles, sometimes to an altitude greater than 1000 km above the magnetic equator. The depletions also map down along the entire magnetic flux tube to $\pm 15^{\circ}$ magnetic latitude. The walls and interiors of these depleted regions are characterized by ionospheric density fluctuations or irregularities over a range of scale sizes from kilometers to centimeters [*Woodman and LaHoz*, 1976; *Basu and Basu*, 1981]. Transionospheric signals passing through the irregularities experience fluctuations in signal amplitude and phase, commonly known as scintillations, which may result

[1]Department of Physics, Raja Peary Mohan College, Uttarpara, India.
[2]S. K. Mitra Center for Research in Space Environment, University of Calcutta, Calcutta, India.

0048-6604/12/2011RS004942

in signal fading, message errors, loss of phase lock in satellite communication systems. In terms of scintillation activity, the region of greatest concern for most users of space based communication and navigation systems is the range of EIA. As the highest levels of electron density on earth persists around the crests of the anomaly, the interaction of the transionospheric radio waves with the bubbles gives rise to intense scintillation activities, both in amplitude and phase around the region [*Whalen*, 2009, and references therein]. In general, all the equatorial stations observe high scintillation activity during the equinoxes, while the minimum activity is recorded during June solstice at the stations in South America, Asia and African sectors and during December solstice at those in Pacific sector [*Aarons et al.*, 1980]. A prominent solar activity dependence, with higher occurrence in high solar activity period, is reflected in the occurrence statistics of scintillation. It may be mentioned that the climatology of equatorial scintillation is fairly well established [*Basu et al.*, 1988; *Aarons*, 1993; *Chakraborty et al.*, 1999], but the weather information of scintillation is a continuing enigma in equatorial aeronomy. The focus of the paper is to develop a forecasting capability for postsunset ionospheric scintillation particularly near the crest of the equatorial anomaly which is globally the most vulnerable region in terms of severity of scintillation.

[4] As for precursors of occurrence of density irregularities, important indices used are (i) strength of EIA at sunset and prior to it [*Raghavarao et al.*, 1988], (ii) $\boldsymbol{E} \times \boldsymbol{B}$ plasma drift velocity around 1830–1900 LT [*Anderson et al.*, 2004], (iii) daytime equatorial electrojet (EEJ) strength [*Haerendel and Eccles*, 1992; *Sastri*, 1998]. *Raghavarao et al.* [1988] showed that the large crest-to-trough ratio of EIA developing in 270–300 km altitude range between 1700 and 1900 LT on the spread-F days is conspicuously absent on non-spread-F days. Using correlation studies, *Li et al.* [2008] also made the similar remark. *Mendillo et al.* [2001] reported that the best available precursor for premidnight ESF is the EIA strength at sunset. A feedback mechanism between a fairly strong EIA at 1700 LT and PRE is supposed to accentuate the irregularity processes [*Prakash et al.*, 2009]. Analyzing total electron content (TEC) values *Thampi et al.* [2008] suggested that ESF tends to occur on the days with well developed and symmetrical EIA on both the hemispheres. Using daytime airglow intensity variations, *Sridharan et al.* [1994] showed that prediction of spread-F is possible three hours in advance. The irregularities occur when the base of the F layer rises to higher altitudes in the evening hours and attains a threshold value [*Farley et al.*, 1970; *Fagundes et al.*, 2009, and references therein]. Using Jicamarca (11.9°S, 76.9°W geographic) Digital Souder data between 1830 and 1930 LT and UHF (250 MHz) scintillation data from Ancon, Peru (11.8°S, 282.9°E geographic) and Antofagasta, Chile (26.7°S, 289.6°E geographic), *Anderson et al.* [2004] reported a threshold drift velocity of 20 m/s to predict S_4 values after 2000 LT, which is suggested to be the necessary and sufficient condition for occurrence of scintillations. In the Indian longitude sector several workers [*Chandra et al.*, 1997; *Dabas et al.*, 2003] confirmed the existence of threshold values of 30 m/s and 20 m/s respectively during high and low sunspot years.

[5] One distinguishing feature of the equatorial ionosphere is the daytime electrojet (EEJ) that refers to the strong E region current in a latitudinal belt of $\pm 2°$ around the magnetic equator [*Chapman*, 1951]. A measure of electrojet yields a proxy of equatorial zonal electric field. The field related to daytime EEJ is reported [*Haerendel and Eccles*, 1992] to have some modulating effect on the ionosphere around the postsunset period. It is proposed that the EEJ current near sunset has a significant role in the determination of the postsunset enhancement of eastward electric field. Using magnetometer and ionosonde data from a chain of stations along the Indian longitude zone, *Sastri* [1998] found a good correspondence between postnoon (1300–1600 LT) EEJ (zonal E region electric field) and postsunset abnormal height rise and subsequent generation of ESF. On the other hand, a striking correlation between longitude structure of postsunset EIA and noontime EEJ is also established. It is suggested [*England et al.*, 2006; *Li et al.*, 2008] to be related to the same large scale modulation of the electric field to affect both systems.

[6] Daytime TEC near the crest of anomaly is very sensitive to EEJ [*Rastogi and Klobuchar*, 1990]. It has been suggested [*Raghavarao et al.*, 1988; *Haerendel and Eccles*, 1992; *Sastri*, 1998; *Sreeja et al.*, 2009] that the PRE is related to the daytime EEJ. But measurement of EEJ requires magnetometers or radars. TEC near the crest of the anomaly may then be taken as a simple and economical proxy index of EEJ which influences the PRE of eastward electric field and hence generation of irregularities at the magnetic equator.

[7] The depth of scintillation, i.e., the amplitude of signal fluctuations is directly related to level of fluctuations in electron density or the integrated electron density deviation ($\int \Delta N dl$) along the raypath. It is controlled by irregularity amplitude ($\Delta N/N$), background electron density (N) and its distribution in the ionosphere. Though the irregularity amplitude does not change much with solar activity [*Basu et al.*, 1988] or from equatorial to anomaly crest region [*de Paula et al.*, 2003], the background ionization density at the anomaly crest undergoes variation by a factor of 10 from high to low solar activity periods [*Anderson et al.*, 1987; *Basu et al.*, 1988]. Near the anomaly crest, persistence of high ambient ionization in the postsunset hours and consequently intense density irregularities are the prerequisites for severe nighttime equatorial scintillation activities under quiet geomagnetic condition [*Anderson and Klobuchar*, 1983; *Chakraborty et al.*, 1999]. Actually, the ambient level around the postsunset period may be assumed to be the combined effect of daytime residual ionization and resurgence of anomaly driven by PRE. TEC is considered to be a measure of ambient ionization. Its diurnal profile is characterized by an increasing trend to attain the diurnal maximum followed by a decaying phase that is occasionally interrupted by the resurgence-like effect induced by the PRE of eastward electric field. The persistence of high residual ionization in the postsunset period should depend on the developing and decaying trends which may be expressed through overall pattern of diurnal TEC profile. The time and amplitude of diurnal maximum, half width, and average level of TEC around the sunset period may be supposed to be important indices to modulate the ambient condition around the postsunset period. If all other conditions such as solar flux, loss factor, etc., on two consecutive days may be

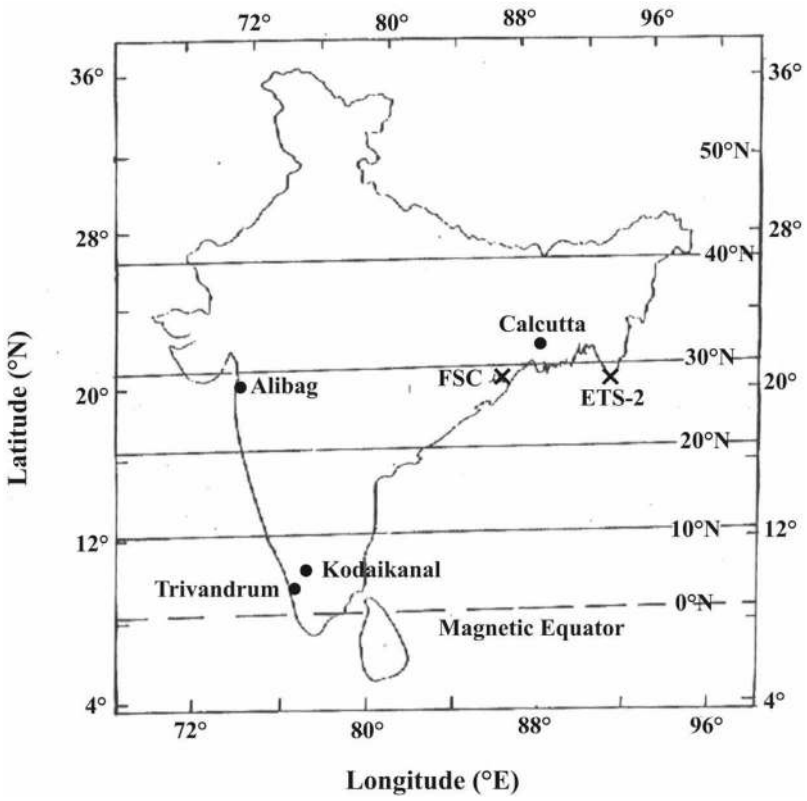

Figure 1. Location of the observing station Calcutta, with respect to the equatorial anomaly crest of the Indian longitude sector. Locations of ionosonde station at Kodaikanal as well as magnetometer stations at Alibag and Trivandrum are also indicated. Geographical latitudes and longitudes are shown. Horizontal lines indicate isodip lines (geomagnetic). Locations of the 400 km subionospheric points of the satellites ETS-2 and FSC paths are also shown by crosses.

assumed to remain more or less the same, the day with higher values of the above parameters will have greater probability of sustenance of higher ambient level in post-sunset period which may further be intensified by the resurgence effect. The aim of the present investigation is to identify parameters of diurnal TEC profile which may be used for forecasting of occurrence of postsunset equatorial VHF/UHF scintillation around the EIA crest under quiet geomagnetic conditions.

2. Data

[8] VHF (136.11 MHz) and UHF (244 MHz) amplitude scintillation data from two satellites ETS-2 (130°E) and Fleet Sat Com (FSC) (73°E), and TEC data recorded at the Ionosphere Field Station, Haringhata (geographic: longitude 88.38°E, latitude 22.58°N, dip: 32°N), University of Calcutta (Figure 1), using the Faraday rotation technique [*Garriott*, 1960; *Goodman*, 1966; *Davies*, 1989] of a VHF (136.11 MHz) transionospheric signal from geostationary satellite ETS-2 (130°E), have been analyzed for the present investigation. The 400 km subionospheric point of ETS-2 path is located at 21°N, 92.7°E (geographic), dip: 27°N and that of FSC is located at 21.1°N, 87.1°E (geographic), dip: 27°N. The subionospheric positions are to the immediate south of the northern crest of EIA. Scintillation data are scaled according to usual "third peak" method [*Whitney et al.*, 1969; *Basu and Basu*, 1989] and fluctuations above 6 dB level are only considered. For information regarding ESF and virtual height of F layer (h′F), ionosonde data, available at 1 h interval, from an equatorial station Kodaikanal (geographic: longitude 77.5°E, latitude 10.25°N, dip: 4°N) are used (Figure 1).

[9] The EEJ data are obtained from the Indian Institute of Geomagnetism (IIG), Mumbai. The strength of EEJ is estimated using the method suggested by *Chandra and Rastogi* [1974]. Accordingly, the hourly variations of the horizontal component (H) of the geomagnetic field relative to its nighttime value at Alibag (ΔH_A) (geographic: longitude 72.87°E, latitude 18.63°N; dip: 23°N) are subtracted from the corresponding values at Trivandrum (ΔH_T) (geographic: longitude 76.57°E, latitude 8.29°N; dip: 1.2°S) for the measurement of EEJ strength, (ΔH_T - ΔH_A). Trivandrum is an EEJ station while Alibag is located outside the EEJ belt (Figure 1).

[10] It may be mentioned that the Ionosphere Field station at Haringhata, ionosonde station at Kodaikanal and magnetometers stations at Trivandrum, Alibag are not exactly situated along the same longitude (Figure 1). There is a longitude difference (∼15°) large enough to show point to point correspondence but the average picture may be assumed to be the same.

[11] Only the data for equinoctial months (February, March, April and August, September, October) of high solar

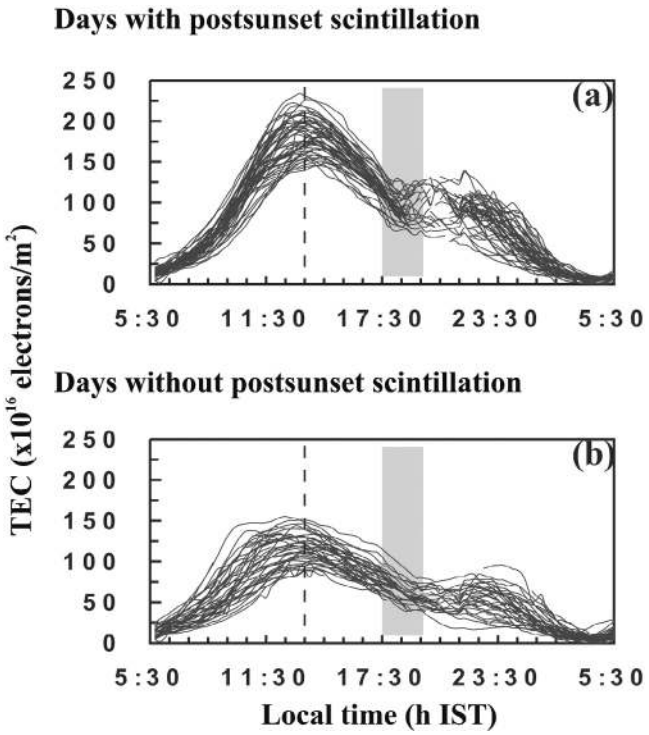

Figure 2. Mass plots of diurnal TEC for (a) days with postsunset scintillation and (b) without scintillation during equinoctial months of 1989–1990. The shaded region indicates the interval around local sunset. Vertical dashed line corresponds to 1330 h IST. In Figure 2a TEC measurement is disrupted in the postsunset period owing to severe scintillation and associated fast polarization fluctuations.

activity period of descending (1980–1981) and ascending (1989–1990) epochs of 21st and 22nd solar cycles are investigated. The days pertaining to geomagnetic disturbances as well as counter electrojet events are not included in the analysis.

3. Results and Discussions

3.1. Diurnal Variation of TEC on Days With and Without Scintillation Events

[12] To diagnose the features of diurnal TEC variations which will differentiate the days with and without scintillation activity, a statistical investigation is made. Figure 2 shows the mass plots of the diurnal TEC profiles during the equinoctial months of high solar activity years (1989–1990). Figure 2a pertains to the days with severe scintillation activities in local postsunset hours. Scintillations in the early evening hours are mostly associated with fast fluctuations of polarization [*DasGupta et al.*, 1982] leading to the disruption of TEC recording. Figure 2b corresponds to the days with no such events. A comparative study of both the panels reveals some distinctive features of diurnal TEC profiles on the scintillation and non-scintillation days. The differences are reflected in (i) diurnal maximum values of TEC (TEC_m), (ii) local times (LT_m) at which diurnal TEC maximizes, (iii) 3-dB width or half width (W_T) of diurnal TEC profile, (iv) integrated TEC values during the daytime hours ($ITEC_d$) (from 0730 to 1730 h IST) (IST, Indian standard time = universal time (UT) + 0530 h), and (v) average TEC level (TEC_{av}) over 2 h-interval centered around local sunset time (from 1 h before sunset to 1 h after sunset). The parameters studied are listed in Table 1 along with corresponding definitions.

[13] On the scintillation days TEC maximizes mostly at or after 1330 h IST, average occurrence time being 1340 h IST. Also, in most of the cases diurnal maximum TEC values are greater than 150 TECU (TEC unit, TECU = 10^{16} electrons/m^2) with 185 TECU as the average maximum value. For non-scintillation days the average maximum TEC value is 120 TECU and the corresponding occurrence time is 1300 h IST. The delayed occurrences of diurnal maximum with higher values are actually indications of strong development of EIA which may lead to a greater probability of persistence of higher ambient level around the sunset period. An indication of the persistence of long-duration higher ambient level may also be reflected if the 3-dB width or half width (W_T) of diurnal patterns is considered in conjunction with diurnal TEC maximum. The parameter thus generated combining the width and diurnal TEC maximum, $C_T = W_T \times TEC_m$, may be helpful to dictate the period of continuation of high ambient level. For days with postsunset scintillation, the average C_T value is recorded to be 1125 TECU-h, while it is about 780 TECU-h for non-scintillation days. The daytime integrated TEC values ($ITEC_d$) and the average TEC levels around the sunset hours (TEC_{av}) are also found to assume significantly larger values on scintillation days (average values being 1360 TECU-h and 97 TECU respectively) compared to the days without postsunset scintillation (940 TECU-h and 67 TECU).

[14] Occurrence of scintillation in the low latitude belt is primarily controlled by the generation, growth and dynamics of scintillation-producing irregularities at the magnetic

Table 1. Parameters of Diurnal TEC and EEJ

Parameter	Definition	Unit
TEC_m	Diurnal maximum value of TEC	TECU
LT_m	Local time of diurnal TEC maximum	h IST
W_T	3-dB width or half width of diurnal TEC profile	h
C_T	$W_T \times TEC_m$	TECU-h
$ITEC_d$	Integrated TEC values during daytime hours (from 0730 to 1730 h IST)	TECU-h
TEC_{av}	Average TEC level over 2 h-interval centered around local sunset time (from 1 h before sunset to 1 h after sunset)	TECU
EEJ_m	Diurnal maximum value of EEJ	nT
W_E	3-dB width or half width of diurnal EEJ profile	h
$IEEJ_d$	Integrated EEJ values during daytime hours (from 0730 to 1730 h IST)	nT-h
$IEEJ_p$	Integrated EEJ values during presunset period (from 2 h to 1 h before sunset)	nT-h

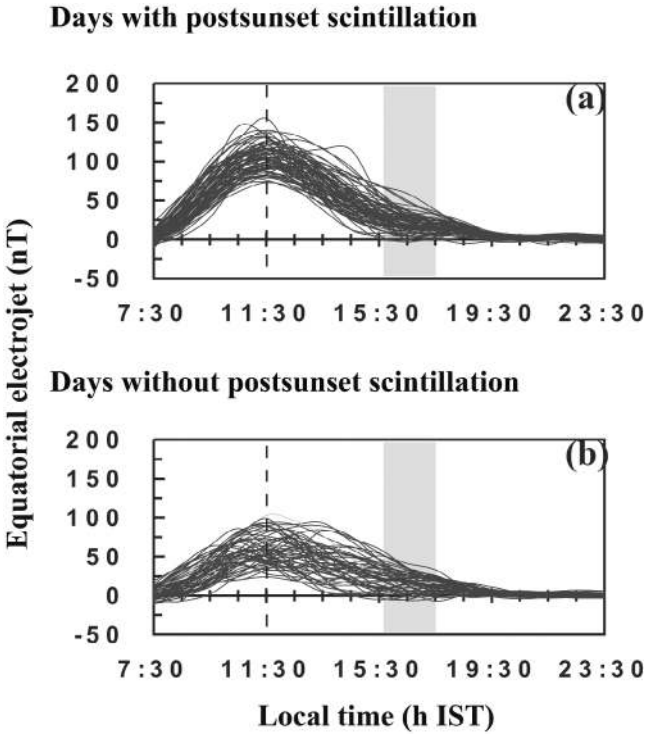

Figure 3. Mass plots showing diurnal variations of EEJ for (a) days with postsunset scintillation and (b) without scintillation. All the data refer to equinoctial months only. The vertical dashed line corresponds to 1130 h IST. Shaded portion indicates the time period from 2 h to 1 h before the local sunset.

equator [*Somayajulu et al.*, 1984]. It was also reported that the evolution of ionosphere through the daytime processes like EIA plays an important role in the generation of ESF [*Thampi et al.*, 2008]. The EIA owes for its evolution and dynamics to the equatorial fountain for which EEJ may be considered as a proxy index [*Anderson et al.*, 2002]. It was suggested [*Haerendel and Eccles*, 1992] that the daytime EEJ flows into the nightside region and that the vertical divergent current of EEJ connects to the vertical F region dynamo current. *Sastri* [1998] and *Dabas et al.* [2003] reported a good positive correlation between the daytime EEJ strength and both h′F and $\boldsymbol{E} \times \boldsymbol{B}$ drift at the evening hours, which are supposed to be important components for evolution of equatorial irregularities [*Fejer et al.*, 1999]. Recently *Sreeja et al.* [2009] reported a plausible linkage of daytime EEJ-related field variations with the PRE, i.e., the occurrence of ESF. The present study concerns with diurnal variation of TEC in the context of forecasting postsunset scintillation near the anomaly crest. As equatorial fountain has a significant contribution to the development of the diurnal TEC profile around the present location, attempts have been made to diagnose suitable EEJ parameters (proxy of equatorial fountain), helpful for dictating higher ambient level near the anomaly crest around the postsunset period susceptible to severe scintillation activities.

[15] The mass plots of diurnal variations of EEJ during equinoctial months of high solar activity years (1989–1990) are shown in Figure 3. Figure 3a pertains to the days with postsunset VHF/UHF scintillation, while Figure 3b presents some days without such events. Diurnal maximum values of EEJ normally reflect the day's EEJ strength vis-à-vis the strength of equatorial fountain. The half width of EEJ in conjunction with diurnal maximum strength may be a signature of the duration of strong fountain. Cumulative effects of equatorial fountain on anomaly parameter may be studied using daytime integrated values of EEJ ($IEEJ_d$). As in case of TEC, the diurnal patterns of EEJ exhibit prominent differences between scintillation and non-scintillation days. Though the differences in local time at which EEJ maximized are not clear in the plots, prominent differences may, however, be reflected in (i) daily maximum values (EEJ_m) of EEJ (ii) 3-dB widths or half widths of daily EEJ profiles (W_E), (iii) integrated EEJ values ($IEEJ_d$) over the period extending from 0730 h IST to 1730 h IST and (iv) integrated EEJ values during presunset period ($IEEJ_p$, from 2 h to 1 h before the sunset) (Table 1). The last one is selected to allow certain time delay for inducing electrodynamic effects of the magnetic equator to the present location.

[16] Thus the study of diurnal TEC profile near the anomaly crest and the diurnal patterns of EEJ identify certain parameters with marked differences in scintillation and non-scintillation days. The parameters are statistically studied in the context of identifying suitable precursor(s) of postsunset scintillation.

3.2. Daytime TEC Parameters and Postsunset Scintillation

[17] Scintillation activities at the present location in the equinoctial months of high solar activity years are primarily the extension of irregularity processes near the magnetic equator. To study the correspondence between the occurrences of equatorial scintillation and the daytime ambient ionization conditions, only the scintillation events preceded by ESF are considered. One shortcoming of ESF data is the lack of identification of type, range or frequency spread-F. However, ESF during postsunset hours of equinoctial months of high solar activity years may be mostly assumed to be range type spread-F to develop scintillation activities [*Rastogi*, 1980; *DasGupta et al.*, 1983].

[18] In Figure 4, variations of TEC_m, C_T, $ITEC_d$, TEC_{av} are plotted against the local times (LT_m) of diurnal TEC maximum during equinoxes of 1989 and 1990. Filled circles correspond to days when both ESF at equatorial station and scintillation at Calcutta are observed, open circles pertain to days with ESF but without scintillation, and crosses represent days without ESF and scintillation. The possibilities of suggesting cut-off/threshold values of the parameters for the occurrences of postsunset scintillation are evident in the plots. A close inspection of Figure 4 reveals the threshold values of (i) 1330 h IST for local time (LT_m) of TEC maximization (vertical dotted lines in each panel of Figure 4), (ii) 130 TECU for maximum values of TEC (TEC_m) (Figure 4a), (iii) 800 TECU-h for C_T parameter (Figure 4b), (iv) 1000 TECU-h for daytime integrated TEC ($ITEC_d$) (Figure 4c) and (v) 75 TECU for average TEC level (TEC_{av}) (Figure 4d) for the occurrences of scintillation. It may be mentioned that statistical test (chi-square (χ^2) test) of correspondence between scintillation occurrence and LT_m is performed considering different values of LT_m. It is observed that the correspondence is significant at the highest level (1%) when threshold value of LT_m is taken as 1330 h IST. The same

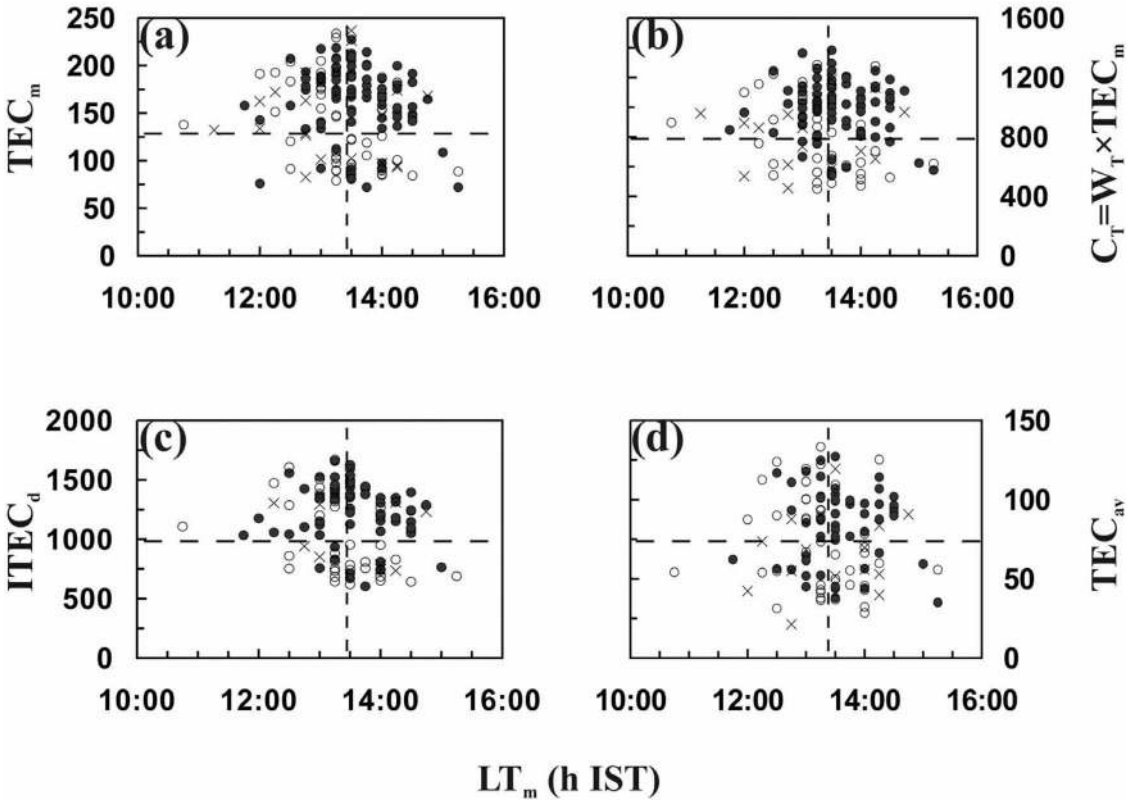

Figure 4. Plots of (a) TEC_m, (b) C_T, (c) $ITEC_d$ and (d) TEC_{av} against local time (LT_m) of diurnal TEC maximum. All the data pertain to equinoctial months. Filled circles correspond to days when both ESF at equatorial station and scintillation at Calcutta are observed, open circles pertain to days with ESF but without scintillation, and crosses represent days without ESF and scintillation. Threshold values of the parameters for the occurrences of scintillation are indicated by the vertical and horizontal dotted lines. First quadrant enclosed by dotted vertical and horizontal lines contains maximum number of scintillation days.

procedure is followed for selecting threshold values of other parameters also. Assuming the above threshold values, individual parameters are separately studied to develop predictive capability of postsunset scintillation events.

3.2.1. Single Parameters of Daytime TEC Profile and Scintillation Probability

3.2.1.1. Local Time (LT_m) of Diurnal TEC Maximum

[19] When the days are grouped according the local time of diurnal TEC maximum (LT_m), postsunset scintillation is found to occur in about 68% of the days on which TEC maximizes at or after 1330 h IST, while on the days with earlier maximization of TEC, scintillation is recorded only 42% cases. Thus, when the criterion of threshold time, 1330 h IST, is not satisfied, probability of non-occurrence of scintillation is 58%. The statistical test for association confirms the correspondence between scintillation occurrence and local time of maximization of TEC at high (1%) significance level. The delayed peak corresponds to greater probability of sustenance of higher ambient level around the postsunset period. It may accentuate the feedback mechanism from EIA to magnetic equator to develop PRE [*Prakash et al.*, 2009] and hence probable irregularity activities.

3.2.1.2. C_T Parameter

[20] Importance of duration of high ambient level may fruitfully be presented by the C_T parameter. All the days of equinoctial months are grouped according to various values of C_T. It is found that for both the solar epochs, the percentage of days exhibiting postsunset scintillation increases with increase in the values of C_T (Figure 5). Considering the threshold values (800 TECU-h) of C_T, as obtained from Figure 4b, it is found that for the days with C_T values equal or larger than 800 TECU-h, postsunset scintillation occurs for 65% cases and 67% of the days with lower C_T values exhibit no scintillation in the postsunset period. A test of significance reveals high level (1%) of association of scintillation occurrence with larger values of C_T.

3.2.1.3. Daytime Integrated TEC ($ITEC_d$)

[21] The intensity of scintillation is controlled by the integrated density deviations (ΔN). A higher background (N) implies larger integrated density deviations (ΔN), hence intense scintillation activities. The higher background condition is the superposition effect of daytime residual ionization and anomaly resurgence contribution due to PRE. The daytime overall ambient level may be a significant contributor to dictate the ionospheric conditions around the sunset period. The diurnal TEC values are integrated throughout the day ($ITEC_d$) from 0730 to 1730 h IST. All the days are grouped according to the various ranges of $ITEC_d$ values and the corresponding percentage occurrences of scintillation are calculated. The results are presented in Figure 6. It appears that the percentage occurrence of postsunset scintillation increases with increase in $ITEC_d$.

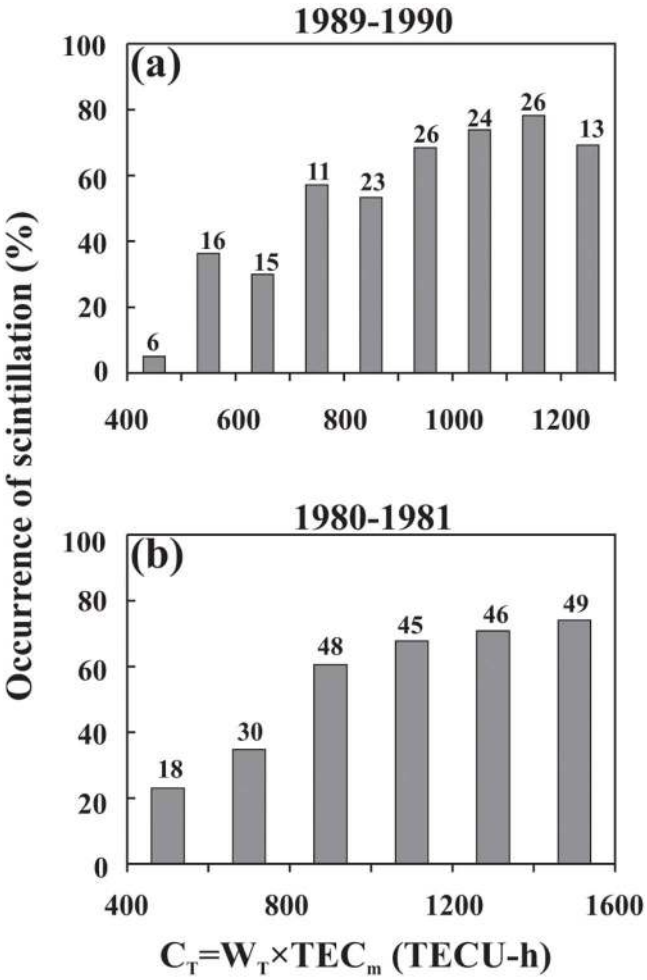

Figure 5. Percentage occurrence of scintillation for different ranges of C_T for two solar epochs, (a) 1989–1990 and (b) 1980–1981. The numbers on the histograms indicate the number of events in the equinoctial months considered.

[22] In the equinoctial months of high solar activity years, 1000 TECU-h may be taken as the threshold value of $ITEC_d$ (Figure 4c) for the occurrence of postsunset scintillation. If $ITEC_d$ is equal or greater than 1000 TECU-h, scintillation is recorded in 71% cases, while it occurs only in 36% cases if $ITEC_d$ < 1000 TECU-h. The result is more or less same for both the solar epochs.

3.2.1.4. Average TEC Level Around Sunset (TEC_{av})

[23] The importance of ionospheric conditions around the sunset period for triggering the irregularity processes has been reported by several workers [*Tsunoda*, 1985; *Raghavarao et al.*, 1988; *Fejer et al.*, 1999; *Valladares et al.*, 2001; *Li et al.*, 2008]. Under present investigation, average TEC values around the sunset period are studied to identify the possible precursor of scintillation.

[24] For each day of equinoctial months, the average TEC values (TEC_{av}) are estimated considering TEC data from 1 h before the sunset to 1 h after the sunset time. The days are categorized in several groups according to estimated TEC_{av} values and the corresponding percentage occurrences of scintillation are estimated (Figure 7). The probability of postsunset scintillation occurrence tends to increase with TEC_{av} for both the phases of the solar cycle.

[25] When the days are separated into two groups, with TEC_{av} greater or less than 75 TECU (Figure 4d), it is found that postsunset scintillation occurs in 50% of the days with TEC_{av} equal or greater than 75 TECU and for TEC_{av} < 75 TECU absence of scintillation was recorded in 68% of the days.

[26] The prediction probability of occurrence and non-occurrence of postsunset scintillation for the equinoctial months of high solar activity years, as discussed above, are summarized in Table 2. A scrutiny of Table 2 suggests that daytime integrated TEC value ($ITEC_d$) may be considered as an efficient predictor of postsunset scintillation. Using the parameter, the maximum forecasting probability of 71% is possible to achieve. For further improvement of the forecasting capability, two parameters of diurnal TEC profile are simultaneously considered.

3.2.2. Double Parameters of Daytime TEC Profile and Occurrence Probability of Scintillation

[27] In this section, the occurrence probability of scintillation is investigated combining two parameters of daytime

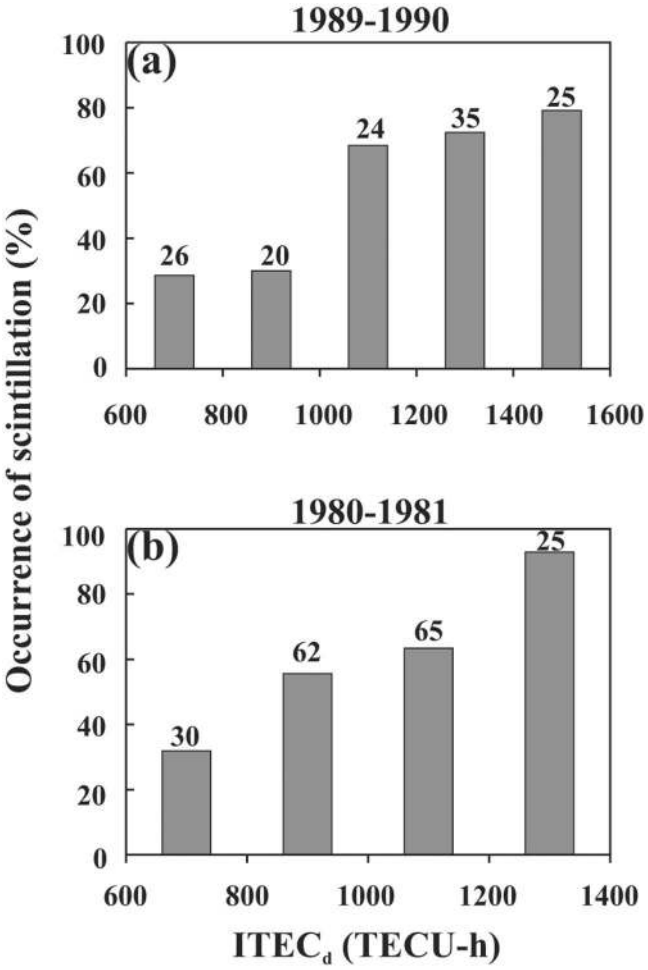

Figure 6. Percentage occurrence of scintillation for different ranges of $ITEC_d$ for two solar epochs, (a) 1989–1990 and (b) 1980–1981. The numbers on the histograms indicate the number of events in the equinoctial months considered.

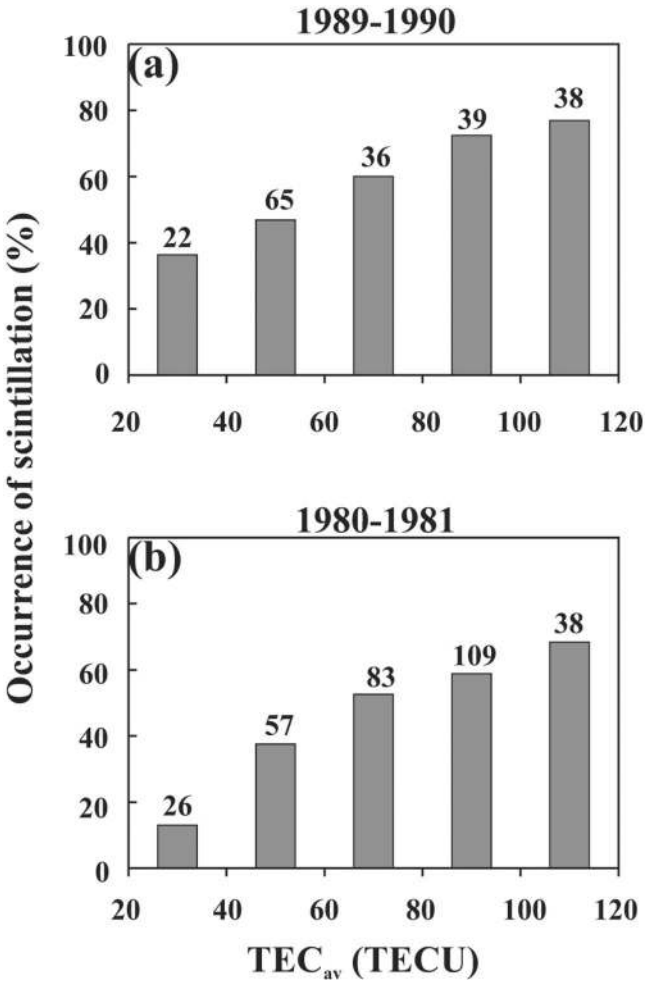

Figure 7. Percentage occurrence of scintillation for different ranges of TEC_{av} for the equinoctial months of two solar epochs, (a) 1989–1990 and (b) 1980–1981. The numbers on the histograms indicate the number of events in the equinoctial months considered.

TEC profile. The statistical analysis revealed that when the occurrence time of diurnal maximum TEC, $LT_m \geq 1330$ h IST, is considered in conjunction with (i) $TEC_m \geq 130$ TECU, (ii) $C_T \geq 800$ TECU-h, (iii) $ITEC_d \geq 1000$ TECU-h or (iv) $TEC_{av} \geq 75$ TECU, the scintillation occurrence probability is greatly enhanced. Also, when both the conditions are simultaneously violated, the non-occurrence probability appears to be more prominent. The pictorial presentation of the extracted results is shown in Figure 8.

[28] The analysis is carried out for equinoctial months of high solar activity years considering all possible combinations of the parameters. The results are summarized in Table 3. In each cell, the first two digits represent the percentage occurrence of postsunset scintillation when both the conditions, as dictated by corresponding row and column headers, are satisfied. The next two digits (separated by "/" from the first two) stand for the percentage of non-occurrence of scintillation when both the criteria are violated simultaneously. The diagonal cells represent the percentage occurrences/non-occurrences of postsunset scintillation for maintaining/violating the single parameter-criterion. Clearly, the prediction efficiency for occurrence as well non-occurrence of scintillation improves noticeably when two parameters, rather than a single TEC parameter, are simultaneously considered. For example, scintillation occurs in 68% cases when TEC maximizes on or after 1330 h IST (LT_m) and in 71% cases when the daytime integrated TEC ($ITEC_d$) is equal or greater than 1000 TECU-h, while simultaneous fulfillment of both the conditions, i.e., $LT_m \geq 1330$ h IST and $ITEC_d \geq 1000$ TECU-h, leads to scintillation occurrence probability of 90%. Thus, observing the local time of diurnal peak and daytime integrated value of TEC simultaneously much ahead of the local sunset (~>1830 h IST), 90% forecasting capability is possible to achieve. Similarly, the prediction probability of non-occurrence of up to 76% is possible to achieve using LT_m and C_T. Clearly, the local time (LT_m) of occurrence of diurnal peak TEC in conjunction with daytime integrated value of TEC ($ITEC_d$) may be considered efficient indices for forecasting the postsunset VHF/UHF scintillation events near the anomaly crest under quiet geomagnetic conditions of high solar activity years. All the results are statistically significant at high levels of significance.

3.3. Scintillation in Relation to Diurnal Variation of EEJ

[29] One of the important factors for triggering equatorial irregularities is the PRE in upward $\boldsymbol{E} \times \boldsymbol{B}$ drift and associated uplifting of the F layer [*Fejer et al.*, 1999]. An estimate of the drift velocity (V_z) may be obtained from the h′F values around sunset [*Bittencourt and Abdu*, 1981]. In Figure 9 the vertical equatorial plasma drift velocity (V_z) around the postsunset hours are plotted against the daytime EEJ parameters (Table 1) for days with and without postsunset scintillation events around the anomaly crest location. All the plots pertain to equinoctial months of high solar activity years (1989, 1990). From the plots, though no apparent relationships between scintillation occurrence, V_z and the EEJ parameters seem to appear, a close inspection of the plots indicates increasing trend of scintillation occurrence with the values of EEJ_m (Figure 9a), C_E ($C_E = W_E \times EEJ_m$) (Figure 9b) and $IEEJ_d$ (Figure 9c), except $IEEJ_p$ (Figure 9d).

[30] For further investigation of the probable correspondence between the daytime EEJ parameters and the postsunset

Table 2. Performances of the Daytime TEC Parameters for the Forecasting of Postsunset Scintillation

	Correct Forecasting of Occurrence of Scintillation (%)	Correct Forecasting of Non-occurrence of Scintillation (%)	Occurrence of Scintillation Without a Forecasting ("Misses") (%)	Non-occurrence of Scintillation Despite a Forecasting ("False Alarm") (%)
LT_m	68	58	42	32
TEC_m	62	60	40	38
C_T	65	67	33	35
$ITEC_d$	***71***	64	36	29
TEC_{av}	50	68	32	50

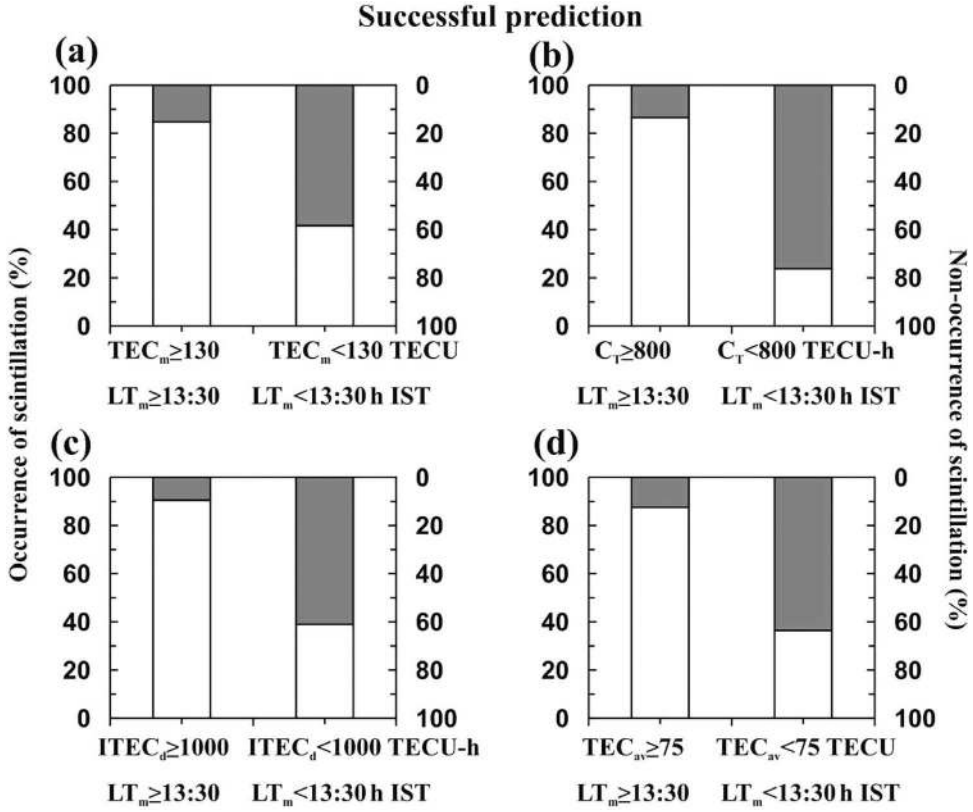

Figure 8. Occurrence probability of equatorial scintillation (shown by white portion) and non-occurrence-probability (shown by shaded part) (right side scale) when dual parameters of diurnal TEC, i.e., (a) LT_m and TEC_m, (b) LT_m and C_T, (c) LT_m and $ITEC_d$, (d) LT_m and TEC_{av} are considered. All the data pertain to equinoctial months.

scintillation events, all the days of equinoctial months of high solar activity years (1989–1990, 1980–1981) are grouped into various ranges of the parameters and the corresponding percentage occurrences of scintillation are estimated (Figure 10). The occurrence probability seems to exhibit a linear trend with EEJ_m (not shown in Figure 10), C_E and $IEEJ_d$, while no such trend is reflected when the integrated EEJ during the presunset period ($IEEJ_p$) are considered. It may be mentioned that very recently *Uemoto et al.* [2010], analyzing ionograms from the equatorial station Chumphon (10.7°N, 99.4°E; 3.3°N magnetic latitude) for the period from November 2007 to October 2008, found no direct relationship between ESF occurrence and daytime-IEEJ while significant correspondence between ESF occurrence frequency and presunset-IEEJ was reported. The contradicting results may be attributed to the peculiar location of the observing station, Calcutta, the solar activity level and seasons. The study of *Uemoto et al.* [2010] pertains to low solar activity years (2007–2008) discarding the seasonal effect.

[31] To relate the equatorial electrodynamical parameter with TEC near the anomaly crest, daytime integrated TEC ($ITEC_d$) values are plotted against the integrated EEJ ($IEEJ_d$) values (Figure 11). Figure 11 pertains to the days with postsunset scintillation events. $ITEC_d$ is found to increase linearly with $IEEJ_d$. The statistical test of significance of the correlation coefficient (R = 0.54) confirms the highest level association between the two. It may be mentioned that from the previous analysis $ITEC_d$ is emerged as the most efficient precursor of postsunset scintillation. On the other hand, with increase in the ranges of $IEEJ_d$, percentage occurrences of postsunset scintillation exhibit an increasing trend. As signature of development of EIA is reflected in the measured values of TEC around the anomaly crest, the statistical correspondence between $IEEJ_d$ and $ITEC_d$ may signify that better forecasting capability may be achieved through the simultaneous consideration of both the parameters. The former pertains to the equatorial electrodynamics, one of the key factors for evolution of density irregularities, and

Table 3. Percentage Occurrence/Non-occurrence of Postsunset Scintillation as Predicted Using Double Parameters of Daytime TEC

	$LT_m \geq 1330$ h IST	$TEC_m \geq 130$ TECU	$C_T \geq 800$ TECU-h	$ITEC_d \geq 1000$ TECU-h	$TEC_{av} \geq 75$ TECU
$LT_m \geq 1330$ h IST	68/58				
$TEC_m \geq 130$ TECU	85/58	62/60			
$C_T \geq 800$ TECU-h	87/***76***	64/68	65/67		
$ITEC_d \geq 1000$ TECU-h	***90***/61	70/66	73/71	71/64	
$TEC_{av} \geq 75$ TECU	88/64	63/62	65/71	71/65	50/68

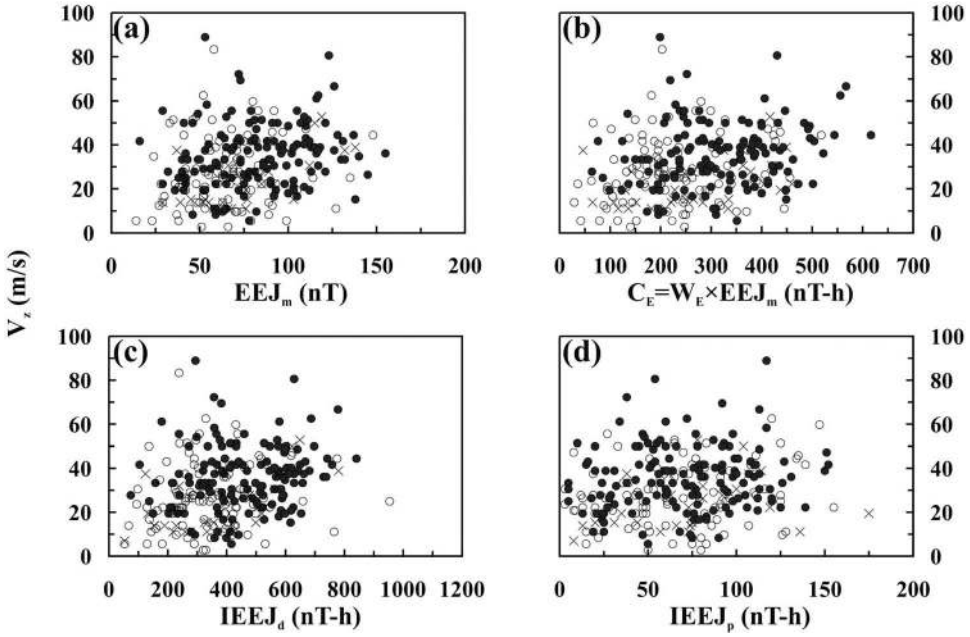

Figure 9. Scatterplots of V_z (m/s) versus (a) maximum EEJ values (EEJ_m) (nT), (b) C_E (nT-h), (c) daytime integrated EEJ ($IEEJ_d$) (nT-h) and (d) integrated EEJ before sunset ($IEEJ_p$) (nT-h). Filled circles correspond to days when both ESF at equatorial station and scintillation at Calcutta are observed, open circles pertain to days with ESF but without scintillation, and crosses represent days without ESF and scintillation. All the data pertain to equinoctial months of high solar activity periods.

the later modulates the effects of irregularities near the anomaly crest. An enhanced value of the later ($ITEC_d$) driven by the field related to higher values of the former ($IEEJ_d$) may develop an environment to enhance the F-to-E region flux tube integrated Pedersen conductivity [*Crain et al.*, 1993] which in turn produces a larger value of eastward electric field and hence prominent PRE effects. It should be mentioned that although, in general, a trend of

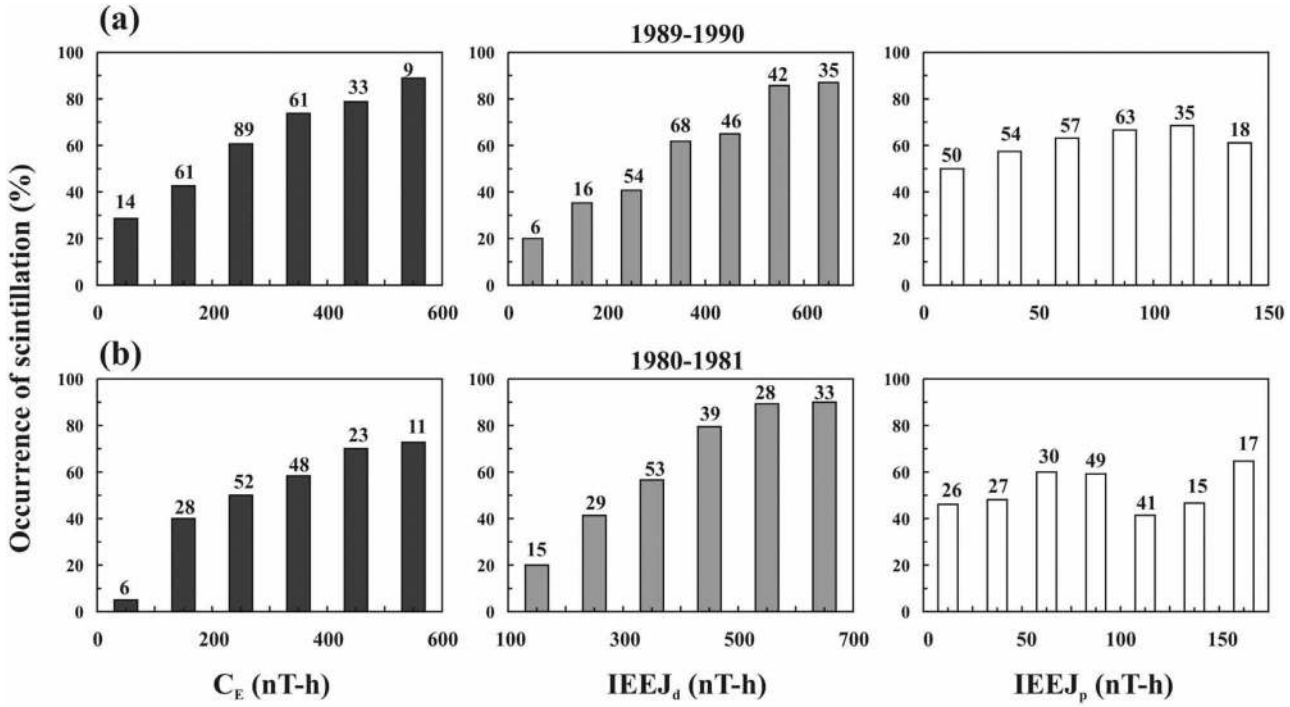

Figure 10. Histograms showing variations of percentage occurrences of scintillation for different ranges of C_E, $IEEJ_d$ and $IEEJ_p$ for equinoctial months of the periods (a) 1989–1990 and (b) 1980–1981.

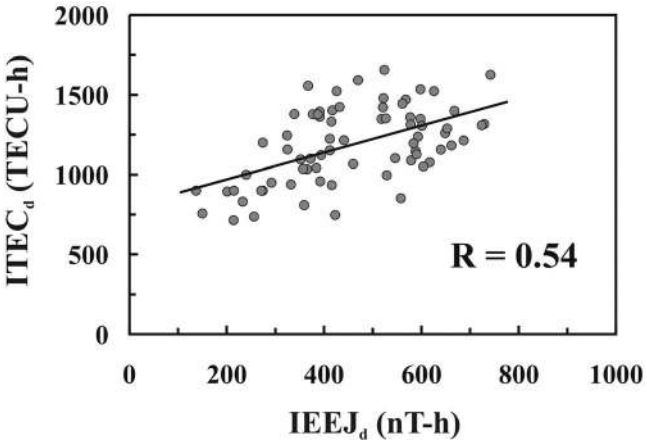

Figure 11. Plots of $ITEC_d$ and $IEEJ_d$ for the days with scintillation activity in the equinoctial months of high solar activity years (1989–1990). A linear trend line with corresponding correlation coefficient (R) is also shown.

correspondence between occurrence probability of scintillation and proxies of equatorial electrodynamics (EEJ) may be observed, no threshold values of the proxies are possible to suggest.

4. Conclusions

[32] In the present investigation, efforts are made to identify the suitable precursors in diurnal TEC profile for postsunset scintillation occurrence near the anomaly crest (Calcutta) during equinoctial months of high solar activity years. Only the equatorial type scintillations which are more frequent and intense in the said period of both the solar epochs (21st and 22nd) are considered. Late occurrence of diurnal TEC maximum in conjunction with higher integrated values of the same are emerged as potentially efficient predictor of postsunset occurrence of equatorial scintillation near the anomaly crest under quiet geomagnetic conditions. Using TEC parameters, 90% prediction capability is possible to achieve. For non-occurrence of scintillation, duration of higher ambient level, as expressed by the C_T parameter, along with the time of diurnal ionization maximum seem to play the dominant role. Using the parameters it is possible to predict the occurrence/non-occurrence of scintillation well in advance of sunset. Larger values of daytime TEC and delayed occurrence and/or longer duration of high TEC values at the present location, situated near the anomaly crest, may be the signatures of the strong development and longer persistence of the EIA during daytime. It may have twofold effects conducive for occurrence of scintillation around the present location. First, it may indicate strong probability of sustenance of higher residual ionization to intensify the anomaly resurgence effect around the local postsunset period. Second, it may modify the neutral wind system to modulate the evolution process of irregularities [*Hedin and Mayr*, 1973]. The eastward zonal winds driven by diurnal tides are strongly decelerated in the regions of enhanced ionization due to higher resistance of ion drag around the anomaly crests during solar maximum epoch. As a result, more heat is deposited around the regions of EIA crests compared to that in the trough region leading to formation of temperature and pressure ridges collocated with the ionization crests [*Raghavarao et al.*, 1991]. The intensity of these ridges is directly related to the intensity and duration of daytime EIA and the diurnal amplitude of the zonal winds. The anomalous latitude distribution of neutral temperature and pressure gives rise to large scale vertical wind profile characterized by upward wind at the temperature (or EIA) crests, downward wind at the trough and equatorward in between, forming a meridional circulation cell. Linear theories as well as nonlinear numerical simulations of equatorial plasma irregularities [*Sekar et al.*, 1994, and references therein] have established that the vertically downward neutral winds or the equatorial winds converging over the magnetic equator enhance the growth rate of the R-T instability and assist the evolution of the plasma bubbles.

[33] It should be mentioned that during the high solar activity years, several other effects (saturation-like effect, etc.) may modulate the variability of ambient ionization. There is a drastic reduction of scintillation occurrence during sunspot minimum while an order of magnitude variation of background ionization density near the anomaly crest from solar maximum to minimum is also the reported fact [*Anderson et al.*, 1987]. Thus to develop a comprehensive forecasting capability of scintillation, a similar exercise should be made during the periods of variable solar activity levels.

[34] **Acknowledgments.** The authors are thankful to Indian Institute of Geomagnetism, Mumbai, for providing magnetometer data and to J. H. Sastri, Indian Institute of Astrophysics, Bangalore, for supplying ionosonde data. The work has been carried out with the financial assistance of ISRO under RESPOND Program.

References

Aarons, J. (1993), The longitudinal morphology of equatorial F-layer irregularities relevant to their occurrence, *Space Sci. Rev.*, *63*, 209–243, doi:10.1007/BF00750769.

Aarons, J., J. P. Mullen, H. E. Whitney, and E. M. MacKenzie (1980), The dynamics of equatorial irregularity patch formation, motion, and decay, *J. Geophys. Res.*, *85*, 139–149, doi:10.1029/JA085iA01p00139.

Abdu, M. A., I. S. Batista, and J. H. A. Sobral (1995), Equatorial ionospheric electric fields during magnetospheric disturbances: Local time/longitude dependences from recent EITS campaigns, *J. Atmos. Terr. Phys.*, *57*, 1065–1083, doi:10.1016/0021-9169(94)00123-6.

Anderson, D. N., and J. A. Klobuchar (1983), Modeling the total electron content observations above Ascension Island, *J. Geophys. Res.*, *88*, 8020–8024, doi:10.1029/JA088iA10p08020.

Anderson, D. N., M. Mendillo, and B. Herniter (1987), A semiempirical low-latitude ionospheric model, *Radio Sci.*, *22*, 292–306, doi:10.1029/RS022i002p00292.

Anderson, D., A. Anghel, K. Yumoto, M. Ishitsuka, and E. Kudeki (2002), Estimating daytime vertical $\boldsymbol{E} \times \boldsymbol{B}$ drift velocities in the equatorial F region using ground-based magnetometer observations, *Geophys. Res. Lett.*, *29*(12), 1596, doi:10.1029/2001GL014562.

Anderson, D. N., B. Reinisch, C. Valladare, J. Chau, and O. Veliz (2004), Forecasting the occurrence of ionospheric scintillation activity in the equatorial ionosphere on a day-to-day basis, *J. Atmos. Sol. Terr. Phys.*, *66*, 1567–1572, doi:10.1016/j.jastp.2004.07.010.

Basu, S., and S. Basu (1981), Equatorial scintillation—A review, *J. Atmos. Terr. Phys.*, *43*, 473–489, doi:10.1016/0021-9169(81)90110-0.

Basu, S., and S. Basu (1989), Scintillation technique for probing ionospheric irregularities, in *WITS Handbook*, vol. 2, edited by C. H. Liu, pp. 128–136, Univ. of Ill., Urbana.

Basu, S., E. MacKenzie, and S. Basu (1988), Ionospheric constrains on VHF/UHF communication links during solar maximum and minimum periods, *Radio Sci.*, *23*, 363–378, doi:10.1029/RS023i003p00363.

Bittencourt, J. A., and M. A. Abdu (1981), A theoretical comparison between apparent and real ionization drift velocities in the equatorial *F* region, *J. Geophys. Res.*, *86*, 2451–2454, doi:10.1029/JA086iA04p02451.

Chakraborty, S. K., A. DasGupta, S. Ray, and S. Banerjee (1999), Long-term observations of VHF scintillation and total electron content near the crest of the equatorial anomaly in the Indian longitude zone, *Radio Sci.*, *34*, 241–255, doi:10.1029/98RS02576.

Chandra, H., and R. G. Rastogi (1974), Geomagnetic storm effects on ionospheric drifts and the equatorial E_s over the magnetic equator, *Indian J. Radio Space Phys.*, *3*, 332–336.

Chandra, H., G. D. Vyas, H. S. S. Sinha, S. Prakash, and R. N. Misra (1997), Equatorial spread-F campaign over SHAR, *J. Atmos. Sol. Terr. Phys.*, *59*, 191–205, doi:10.1016/1364-6826(95)00199-9.

Chapman, S. (1951), The equatorial electrojet as deduced from the abnormal electric current distribution above Hucancayo and else where, *Arch. Meteorol. Geophys. Bioklimatol., Ser. A*, *4*, 368–390, doi:10.1007/BF02246814.

Crain, D. J., R. A. Heelis, and G. J. Bailey (1993), Effects of electric coupling on equatorial ionospheric plasma motions: When is the F region a dominant driver in the low-latitude dynamo?, *J. Geophys. Res.*, *98*, 6033–6037, doi:10.1029/92JA02195.

Dabas, R. S., L. Singh, D. R. Lakshmi, P. Subramanyam, P. Chopra, and S. C. Garg (2003), Evolution and dynamics of equatorial plasma bubbles: Relationships to $\boldsymbol{E} \times \boldsymbol{B}$ drift, postsunset total electron content enhancements, and equatorial electrojet strength, *Radio Sci.*, *38*(4), 1075, doi:10.1029/2001RS002586.

DasGupta, A., M. C. Lee, and J. A. Klobuchar (1982), VHF Faraday polarization fluctuations and strong L-band amplitude scintillations near Appleton anomaly crest, *Nature*, *298*, 354–357, doi:10.1038/298354a0.

DasGupta, A., S. Basu, J. Aarons, J. A. Klobuchar, S. Basu, and A. Bushby (1983), VHF amplitude scintillations and associated electron content depletions as observed at Arequipa, Peru, *J. Atmos. Terr. Phys.*, *45*, 15–26, doi:10.1016/S0021-9169(83)80003-8.

Davies, K. (1989), Earth-space propagation, in *Ionospheric Radio*, chap. 8, pp. 260–311, Peter Peregrinus, London.

de Paula, E. R., F. S. Rodrigues, K. N. Iyer, I. J. Kantor, M. A. Abdu, P. M. Kinter, B. M. Ledvina, and H. Kil (2003), Equatorial anomaly effects on GPS scintillations in Brazil, *Adv. Space Res.*, *31*, 749–754, doi:10.1016/S0273-1177(03)00048-6.

England, S. L., S. Maus, T. J. Immel, and S. B. Mende (2006), Longitudinal variation of the *E* region electric fields caused by atmospheric tides, *Geophys. Res. Lett.*, *33*, L21105, doi:10.1029/2006GL027465.

Fagundes, P. R., J. R. Abalde, J. A. Bittencourt, Y. Sahai, R. G. Francisco, V. G. Pillat, and W. L. C. Lima (2009), F layer postsunset height rise due to electric field prereversal enhancement: 2. Traveling planetary wave ionospheric disturbances and their role on the generation of equatorial spread F, *J. Geophys. Res.*, *114*, A12322, doi:10.1029/2009JA014482.

Farley, D. T., B. B. Balsley, R. F. Woodman, and J. P. McClure (1970), Equatorial spread F: Implications of VHF radar observations, *J. Geophys. Res.*, *75*, 7199–7216, doi:10.1029/JA075i034p07199.

Farley, D. T., E. Bonelli, B. G. Fejer, and M. F. Larsen (1986), The prereversal enhancement of the zonal electric field in the equatorial ionosphere, *J. Geophys. Res.*, *91*, 13,723–13,728, doi:10.1029/JA091iA12p13723.

Fejer, B. G., E. R. de Paula, S. A. Gonzalez, and R. F. Woodman (1991), Average vertical and zonal F region plasma drifts over Jicamarca, *J. Geophys. Res.*, *96*, 13,901–13,906, doi:10.1029/91JA01171.

Fejer, B. G., L. Scherliess, and E. R. de Paula (1999), Effects of the vertical plasma drift velocity on the generation and evolution of equatorial spread F, *J. Geophys. Res.*, *104*, 19,859–19,869, doi:10.1029/1999JA900271.

Garriott, O. K. (1960), The determination of ionospheric total electron content and distribution from satellite observation: 1. Theory of the analysis, *J. Geophys. Res.*, *65*, 1139–1150, doi:10.1029/JZ065i004p01139.

Goodman, J. M. (1966), Analysis of electron content errors introduced through use of a simplified Faraday rotation technique, *Rep. 1684*, Nav. Res. Lab., Washington, D. C.

Haerendel, G., and J. V. Eccles (1992), The role of the equatorial electrojet in the evening ionosphere, *J. Geophys. Res.*, *97*, 1181–1192, doi:10.1029/91JA02227.

Hedin, A. E., and H. G. Mayr (1973), Magnetic control of the near equatorial neutral thermosphere, *J. Geophys. Res.*, *78*, 1688–1691, doi:10.1029/JA078i010p01688.

Kil, H., and S.-J. Oh (2011), Dependence of the evening prereversal enhancement of the vertical plasma drift on geophysical parameters, *J. Geophys. Res.*, *116*, A05311, doi:10.1029/2010JA016352.

Li, G., B. Ning, L. Liu, B. Zhao, X. Yue, S.-Y. Su, and S. Venkatraman (2008), Correlative study of plasma bubbles, evening equatorial ionization anomaly, and equatorial prereversal $\boldsymbol{E} \times \boldsymbol{B}$ drifts at solar maximum, *Radio Sci.*, *43*, RS4005, doi:10.1029/2007RS003760.

Mendillo, M., J. Meriweather, and M. Biondi (2001), Testing the thermospheric neutral wind suppression mechanism for day-to-day variability of equatorial spread F, *J. Geophys. Res.*, *106*, 3655–3663, doi:10.1029/2000JA000148.

Ossakow, S. L. (1981), Spread-F theories—A review, *J. Atmos. Terr. Phys.*, *43*, 437–452, doi:10.1016/0021-9169(81)90107-0.

Park, J., H. Luhr, B. G. Fejer, and K. W. Min (2010), Duskside *F* region dynamo currents: Its relationship with prereversal enhancement of vertical plasma drift, *Ann. Geophys.*, *28*, 2097–2101, doi:10.5194/angeo-28-2097-2010.

Prakash, S., D. Pallamraju, and H. S. S. Sinha (2009), Role of the equatorial ionization anomaly in the development of the evening prereversal enhancement of the equatorial zonal electric field, *J. Geophys. Res.*, *114*, A02301, doi:10.1029/2007JA012808.

Raghavarao, R., M. Nageswararao, J. H. Sastri, G. D. Vyas, and M. Sriramarao (1988), Role of equatorial ionization anomaly in the initiation of equatorial spread F, *J. Geophys. Res.*, *93*, 5959–5964, doi:10.1029/JA093iA06p05959.

Raghavarao, R., L. E. Wharton, N. W. Spencer, H. G. Mayr, and L. H. Brace (1991), An equatorial temperature and wind anomaly (ETWA), *Geophys. Res. Lett.*, *18*, 1193–1196, doi:10.1029/91GL01561.

Rastogi, R. G. (1980), Seasonal and solar cycle variations of equatorial spread-F in the American zone, *J. Atmos. Terr. Phys.*, *42*, 593–597, doi:10.1016/0021-9169(80)90093-8.

Rastogi, R. G., and J. A. Klobuchar (1990), Ionospheric electron content within the equatorial F2 layer anomaly belt, *J. Geophys. Res.*, *95*, 19,045–19,052, doi:10.1029/JA095iA11p19045.

Rishbeth, H. (1971), Polarization fields produced by winds in the equatorial *F* region, *Planet. Space Sci.*, *19*, 357–369, doi:10.1016/0032-0633(71)90098-5.

Sastri, J. H. (1998), On the development of abnormally large postsunset upward drift of equatorial F region under quiet geomagnetic conditions, *J. Geophys. Res.*, *103*, 3983–3991, doi:10.1029/97JA02649.

Sekar, R., R. Suhasini, and R. Raghavarao (1994), Effects of vertical winds and electric fields in the nonlinear evolution of equatorial spread F, *J. Geophys. Res.*, *99*, 2205–2213, doi:10.1029/93JA01849.

Somayajulu, Y. V., S. C. Garg, R. S. Dabas, L. Singh, T. R. Tyagi, B. Lokanadham, S. Ramakrishan, and G. Navneeth (1984), Multistation study of nighttime scintillations in low latitudes: Evidence of control by equatorial F region irregularities, *Radio Sci.*, *19*, 707–718, doi:10.1029/RS019i003p00707.

Sreeja, V., C. V. Devasia, S. Ravindran, and T. K. Pant (2009), Observational evidence for the linkage of equatorial electrojet (EEJ) electric field variations with the post sunset *F* region electrodynamics, *Ann. Geophys.*, *27*, 4229–4238, doi:10.5194/angeo-27-4229-2009.

Sridharan, R., D. Pallamraju, R. Raghavarao, and P. V. S. Ramarao (1994), Precursor to equatorial spread-F in OI 630.0 nm dayglow, *Geophys. Res. Lett.*, *21*, 2797–2800, doi:10.1029/94GL02732.

Thampi, S. V., S. Ravindran, T. K. Pant, C. V. Devasia, and R. Sridharan (2008), Seasonal dependence of the "forecast parameter" based on the EIA characteristics for the prediction of equatorial spread F (ESF), *Ann. Geophys.*, *26*, 1751–1757, doi:10.5194/angeo-26-1751-2008.

Tsunoda, R. T. (1985), Control of the seasonal and longitudinal occurrence of equatorial scintillations by the longitudinal gradient in integrated E region Pedersen conductivity, *J. Geophys. Res.*, *90*, 447–456, doi:10.1029/JA090iA01p00447.

Uemoto, J., T. Maruyama, S. Saito, M. Ishii, and R. Yoshimura (2010), Relationships between pre-sunset electrojet strength, pre-reversal enhancement and equatorial spread-F onset, *Ann. Geophys.*, *28*, 449–454, doi:10.5194/angeo-28-449-2010.

Valladares, C. E., S. Basu, K. Groves, M. P. Hagan, D. Hysell, A. J. Mazzella, and R. E. Sheehan (2001), Measurement of the latitudinal distribution of TEC during ESF events, *J. Geophys. Res.*, *106*, 29,133–29,152, doi:10.1029/2000JA000426.

Whalen, J. A. (2009), The linear dependence of GHz scintillation on electron density observed in the equatorial anomaly, *Ann. Geophys.*, *27*, 1755–1761, doi:10.5194/angeo-27-1755-2009.

Whitney, H. E., J. Aarons, and C. Malik (1969), A proposed index for measuring ionospheric scintillations, *Planet. Space Sci.*, *17*, 1069–1073, doi:10.1016/0032-0633(69)90114-7.

Woodman, R. F., and C. LaHoz (1976), Radar observations of F region equatorial irregularities, *J. Geophys. Res.*, *81*, 5447–5466, doi:10.1029/JA081i031p05447.

S. K. Chakraborty and R. Hajra, Department of Physics, Raja Peary Mohan College, Uttarpara 712258, India. (skchak2003@yahoo.com)

A. DasGupta, S. K. Mitra Center for Research in Space Environment, University of Calcutta, Calcutta 700009, India.